Open Journal of Fluid Dynamics, 2022, 12, 213-229
https://www.scirp.org/journal/ojfd
ISSN Online: 2165-3860
ISSN Print: 2165-3852

Spin Hydrodynamic Power Generation and Its Influence on Magnetohydrodynamic Effects

Fabiano Sene, Carlos Caicedo, Babak Fahimi

Department of Electrical and Computer Engineering, University of Texas at Dallas, Richardson, USA
Email: fahimi@utdallas.edu

How to cite this paper: Sene, F., Caicedo, C. and Fahimi, B. (2022) Spin Hydrodynamic Power Generation and Its Influence on Magnetohydrodynamic Effects. *Open Journal of Fluid Dynamics*, **12**, 213-229.
https://doi.org/10.4236/ojfd.2022.122010

Received: April 14, 2022
Accepted: June 13, 2022
Published: June 16, 2022

Abstract

This paper reports on generation of electric power using Spin Hydrodynamics (SHD) and its impact on magneto hydrodynamics (MHD). The targeted system uses saltwater as conducting fluid in a channel that is equipped with high energy permanent magnets in that the direction of magnetic field is perpendicular to that of the working fluid. By measuring the induced voltage caused by turbulent motion of conducting fluid (with and without magnetic field) the relationship between the SHD and MHD has been investigated. This system has been further simulated and experimentally verified to validate the claims.

Keywords

Spin Hydrodynamics, Magneto Hydrodynamics, Energy Harvesting

1. Introduction

Inverse Spin Hall Effect (ISHE) across a channel carrying a flow of liquid metals is capable of inducing an electric field [1]. Advances in manipulation of spin currents in [2], discovery of the Spin Nernst Effect in [3] as well as posterior observations on spin quantities relating to the control of electrical quantities through spin manipulation [4] have collectively formed the basis of the emerging field of Spin Hydrodynamics (SHD) and spintronics.

Spin-vorticity coupling has established an opportunity in the field of SHD for energy harvesting using liquid metals and liquid alloys at room temperature [1]. On this subject, the most important discovery is the possibility to harvest electricity from a conductive fluid flow by taking advantage of its charged particles' spin in conjunction with mechanical angular momentum, *i.e.* taking vortices' induction, as a fundamental source, which may then pave a pathway to the design of power generators based on SHD [5].

It is necessary to understand the fundamentals of the system to create ideal conditions for the energy conversion process and to develop an efficient SHD based energy harvesting. **Figure 1** illustrates the steps whereby SHD energy conversion process occurs.

Magnetohydrodynamics comprises of the studies regarding the behavior of electrically conductive fluid flows through externally imposed magnetic fields [6]. This term represents an evolution of the so-called "magneto-electric induction" process, described by Michael Faraday in reference to his famous experiment, wherein the main purpose was to prove that Thames river fluid flow through the geomagnetic field could cause a deflection in a galvanometer [7].

The challenges related to effective use of MHD included high temperature operation caused by the usage of hot plasma, magnetic fields in the order of 5T, and materials that could withstand such an extreme condition during extensive periods. Velikhov *et al.*, mentioned about the Sakhalin MHD facility with 500 MW of installed power in detailed dimensions and operation times.

Nonetheless, the impracticability of MHD generators in large scale underpins the need for advances in material science, more specifically, the development of new materials that can withstand operating temperatures close to 3000 K for extended periods of time, or the synthetization of new fluid metal alloys which facilitate the operation at lower temperatures [8]. Hence, the block diagram in **Figure 2** describes the principles and dynamics of a MHD generator in accordance with the energy conversion process enabled by the Faraday's Law of Induction.

To begin with, MHD and SHD appear as two different phenomena that are independent from each other. However, the most important quantity in SHD, so-called "spin", is simply another degree of freedom that is to be considered in the behavior of fundamental particles, *i.e.* the electrons themselves. In addition, even ions may exhibit a non-zero spin behavior. The implication is that these particles would experience the effects imposed by the flux lines under magnetic fields' influence.

In the context of a MHD energy harvesting device and by allowing the added

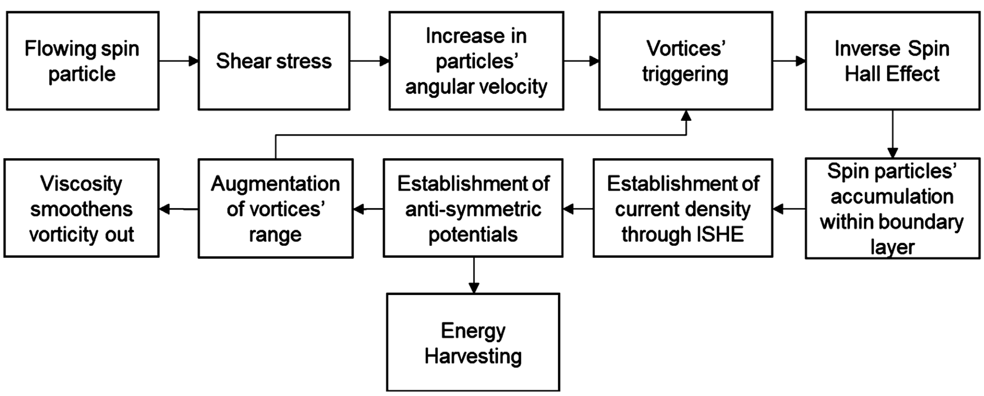

Figure 1. Dynamics of the SHD energy conversion process.

degree of freedom due to spin, the presence of these flowing charged particles implies that they will not only experience the effects of Lorentz Force, but will also be susceptible to the tendency in alignment of the particles' spin with magnetic flux lines. Evidently, the dynamics of particles accumulation across the channel walls will be biased by Stern-Gerlach Force [9].

Moreover, it is crucial to mention that Lorentz and Stern-Gerlach forces have the same nature, but introduce different influences towards the behavior of charged spin particles [10]. On the basis of this operation, as a form to illustrate the process of interference occurring between SHD and MHD within the same system, **Figure 3** depicts the steps whereby energy conversion would occur.

The present paper aims to shed light on the coupling between SHD and MHD through a series of analytical and experimental studies. The main goal is to establish the existence of such couplings and their dependency on various design parameters and operating conditions.

2. Mathematical Modeling

In consonance with the findings claimed in Takahashi *et al.* *[1]*, direct and inverse Hall effect spin currents can be converted into electrical currents by virtue of spin-vorticity coupling [11]. Notably, for the phenomena related to Spin Hydrodynamic to occur based on spin-orbit coupling (SOC) or spin-vorticity coupling [12], it is necessary to take into consideration the spin degree of freedom

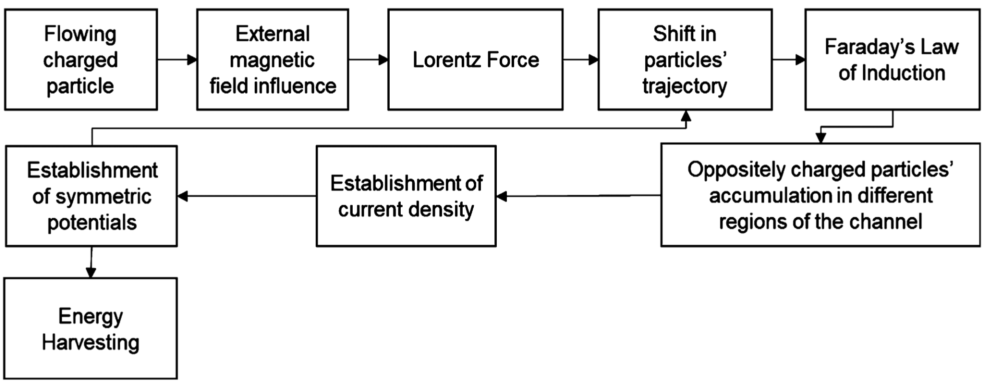

Figure 2. Dynamics of the MHD energy conversion process.

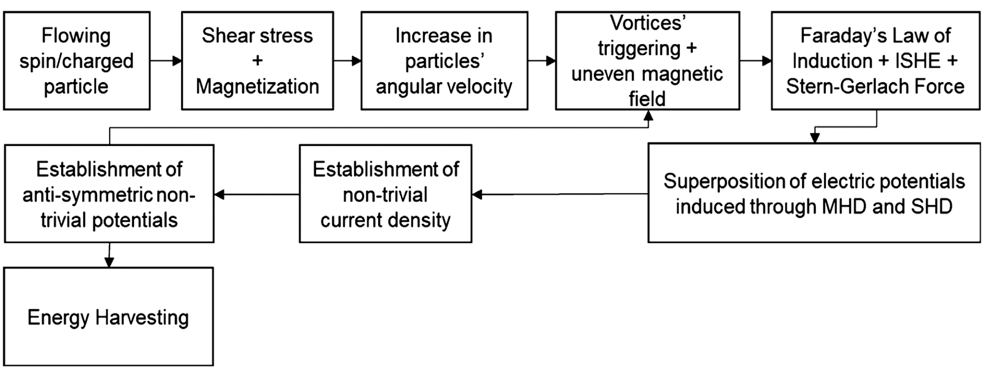

Figure 3. Dynamics of the combined MHD-SHD energy conversion process.

for the analysis of the system.

With a view to imbue clarity regarding SHD, let us consider a pure and electrically conductive fluid to flow under no external electrical or magnetic effects. Moreover, this fluid flow is assumed to be non-ideal, is governed by a velocity profile similar to the Poiseuille flow [13], has a definite viscosity, and is not subject to tribo-electrification [14]. The uneven velocity distribution across the channel can be attributed to the shear stress, known as fluid-structure interaction, which tends to drag the flowing particles in the opposite direction of their flow. With the development of fluid flow, both viscosity and normal stresses take place and tend to induce vorticity, which can be calculated as stated by Equation (1) [15].

$$\boldsymbol{\Omega} = \nabla \times \boldsymbol{U} \tag{1}$$

where $\boldsymbol{\Omega}$ denotes the local vorticity, which is a function of the velocity profile given by $\boldsymbol{U} = \boldsymbol{U}(x, y, z)$. As illustrated in **Figure 4**, it can be observed that the magnitude of the velocity U near the walls gets smaller due to the shear stress. It also causes an increment in the shear stress, consequently inducing local vorticity [15] [16].

Furthermore, the fluid flow is analyzed at three different instants from **Figure 4-left** towards **Figure 4-right**. Evidently, the fluid flow gets developed with the passage of time. The surface levels indicate that the vorticity across the channel boundaries decrease over time.

Considering the fact that the flow is bounded, the net direction of rotation in both (left and right) sides is in opposite direction to one another. In physical terms, this difference of orientation, which relies on the Spin-Orbit Coupling (SOC), has a direct effect in the spin polarization of electron as well as other flowing particles. In an electrically conductive fluid flow, this opposite spin polarization induces what is known as spin accumulation, giving rise to non-trivial anti-symmetric potentials. **Figure 5** shows the manner in which this accumulation occurs, following the anticipated Direct and Inverse Spin Hall effects.

This condition implies that the spin orientation can be attributed to the particles as they get caught within whirls induced in a fluid flow. In the case of a fluid flow, these whirls may be induced due to the shear stress between the channel walls and the fluid, which acts as a trigger for vortices and creates local differences of vorticity.

Hence, it is shown that the bridge between spin and orbital angular momentum is given by the rotational viscosity as well as either Direct or Inverse Spin Hall Effect (ISHE). In terms of energy conversion, the occurrence of ISHE provides a path to translate rotational energy into electrical potential, which makes

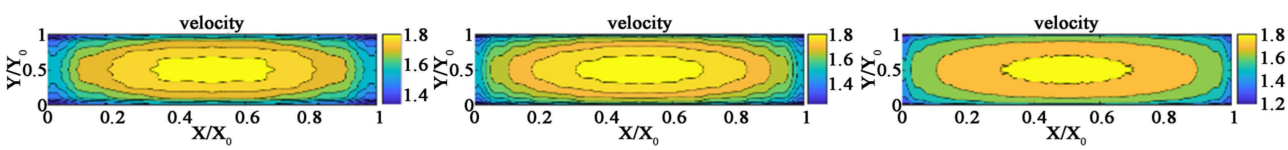

Figure 4. (left) First, (center) second and (right) third instants of the fluid flow profile over time.

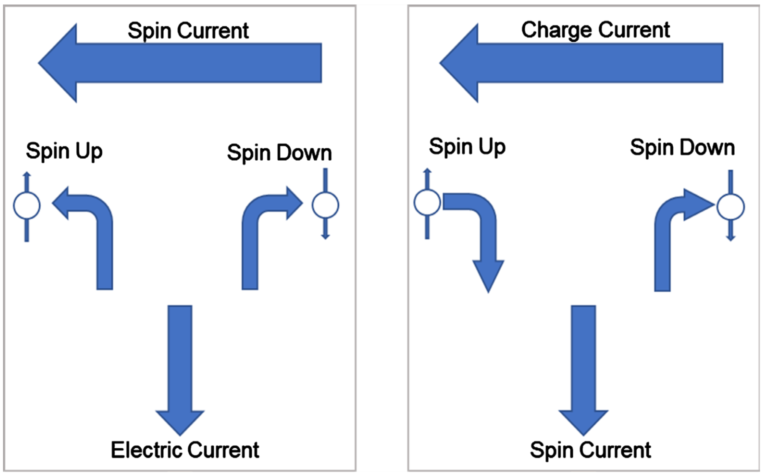

Figure 5. Direct and inverse spin hall effects [4].

it possible to observe this phenomenon with electric probes [17] [18] [19] [20].

Furthermore, once the fluid flow gets developed and the spin particle maintains its rotating movement, it will reduce its rotation radius gradually. Viscosity may play an important role in smoothing that rotational movement. At the very moment when viscosity starts acting, this spin particle still has energy to keep spinning, considering the real limits in a fluid flow. However, its velocity or angular acceleration starts decreasing. Viscosity prevents the particle from spinning with an infinitely high angular velocity due to the intermolecular forces of the fluid.

The fact that this particle, regardless of the viscosity effect, keeps rotating, may characterize a reaction potential to counteract other forces that prevent it from maintaining its rotating movement. This, in turn, can be attributed to the energy that maintains spin polarization. Therefore, it can be inferred that spin polarization is considered as the orientation of the vector intrinsic energy flux contained by the spin particle.

In every device that converts any kind of energy into electrical energy, there are preconditions stated by Maxwell's equations. In terms of voltage induction and electromagnetic excitation of an energy converter, the observance to Faraday's Law of Induction is the first feature. It plays a fundamental role since it determines how the variation of magnetic field will allow for induction of an electric field over time and, consequently, the establishment of a gradient of electric potential across the region under analysis.

Based on these premises, Equation (2) and (3) mathematically elucidate what is the interdependence between electric and magnetic fields towards voltage induction and the establishment of current densities. Meanwhile, Equation (3a) describes the Ohm's Law in conductive fluids, thus indicating that dependence of a moving fluid exposed to external magnetic fields and an eventual electric field is induced due to Joule losses.

$$\nabla \times \boldsymbol{E} = -\frac{\partial \boldsymbol{B}}{\partial t} \tag{2}$$

$$\nabla \times \boldsymbol{B} = \mu \boldsymbol{J} \tag{3}$$

$$\boldsymbol{J} = \sigma\left(\boldsymbol{E} + \boldsymbol{u} \times \boldsymbol{B}\right) \tag{3a}$$

Since the working fluid is a conductive, viscous, and impure fluid, other molecules also exist, albeit in a smaller proportion when compared to its main composition. This explains the capability of energy transfer from particle to the particle contained in the working fluid. In particular, the fact that it has a non-zero electrical conductivity establishes the benchmark to enhance the likelihood that energy transfer phenomena related to sparse electric potentials throughout the medium can indeed play an important role in an energy harvesting system.

As described through Equation (3a), electric current density in fluids is defined as a function of electrical conductivity, applied electric field, fluid velocity, and the magnetic field applied externally. However, for Spin Hydrodynamics purposes, the magnetic field is excluded in order to start conditioning the system from its main feature: spin-vorticity coupling. Furthermore, there is no externally applied electric field that could eliminate Equation (2). Therefore, the sole origin for spin current accumulation is the shear stress induced by the interaction between fluid flow and channel walls.

Given the electrical conductivity σ, it is possible to split it into two terms, as illustrated by Equation (4).

$$\sigma = \sigma_0 + \sigma_{\uparrow\downarrow} \tag{4}$$

where σ_0 is the intrinsic conductivity of the fluid and $\sigma_{\uparrow\downarrow}$ represents the conductivity induced by the shear stress in certain regions of the fluid flow measured in S/m. Moreover, it is noteworthy that, whenever shear stress is considered as a quantity of major importance, viscosity and fluid velocity in close vicinity of the walls will play a role as well.

By splitting viscosity into two components, namely kinematic ν and turbulent ν_t components, (as shown by Equation (5)), it is possible to describe a dimensionless coefficient κ after dimensional analysis, which helps determines the intensity of spin current accumulation. Considering density of the fluid ρ, shear stress τ (a function of the fluid velocity pattern), and the spin diffusion distance λ, Equation (6) can be reached.

$$\nu_{eff} = \nu + \nu_t \tag{5}$$

$$\kappa = \frac{\nu + \nu_t}{\lambda}\sqrt{\frac{\rho}{\tau}} \tag{6}$$

where κ denotes the quantity determining the degree of influence of the spin-orbit coupling in terms of energy harvesting. This quantity depends on the shear stress of the fluid flow. Given the assumption that fluid flow lacks a uniform profile, two different fluid flow profiles will be observed throughout the channel section. The estimation of this parameter is made by taking into consideration the capability of spin for those flowing particles to get diffused within a certain distance, *i.e.* spin diffusion length, and the energy carried by them, as explained in [21] [22]. Accordingly, it is possible to compute an effective value for the conductivity:

$$\sigma_{eff} = \frac{\sigma_0}{\kappa} \tag{7}$$

Equation (4) suggests that the particles' spin equals to $\hbar/2$, diffused within a distance λ, throughout a conductive fluid and effective viscosity ν under a flow condition that is susceptible to the vorticity induction ω due to the salient cylindrical electrodes that are in contact with the fluid flow. It is shown to induce an electric field and consequently, a voltage between these electrodes, an accumulation of spin particles in close proximity to the channel walls is necessary. Equation (9) shows the spin voltage measured by integrating the electric field Equation (8) stated as follows.

$$E_{\uparrow\downarrow} = \hbar \frac{1}{4\pi\varepsilon r^2} \frac{\sigma\upsilon}{|e|\omega\lambda}\left(\frac{u_k}{u}\right) \tag{8}$$

$$V_{\uparrow\downarrow} = -\frac{1}{4\pi\varepsilon r}\left[\frac{\hbar\sigma\nu}{\omega\lambda|e|}\left(\frac{u_k}{u}\right)\right] \tag{9}$$

In order to quantify the active power that can be extracted from this system, and in effect, the system efficiency, Equation (10) is stated as a means of computing the power per unit density.

$$P_{\uparrow\downarrow} = J_{\uparrow\downarrow} E_{\uparrow\downarrow} \tag{10}$$

Similar to power density in electric systems, which is related to the induced current density and electric field, *e.g.* in MHD generators, it is reasonable to analyze the SHD system in terms of current density, which would result from the effective electric conductivity of the working fluid.

$$J_{\uparrow\downarrow} = \frac{\sigma_0}{\kappa} E_{\uparrow\downarrow} = \left[\frac{\sigma_0}{\frac{\nu}{\lambda}\sqrt{\frac{\rho}{\tau}}}\right] E_{\uparrow\downarrow} \tag{11}$$

where σ_0 is the intrinsic electrical conductivity of the fluid in S/m, $E_{\uparrow\downarrow}$ denotes the intrinsic spin electric field, which accounts for the strength of the spin-orbit coupling of the given fluid, κ represents the coefficient scaling the current density in terms of the shear stress in the targeted region, ρ signifies the fluid density, $\hbar$ is the reduced Planck's constant, λ denotes the spin diffusion distance, and ν is the kinematic viscosity of the fluid. Therefore, if the relevant parameters are known it is possible to reach the Equation (12), using which the power density of this device can be computed by combining Equations (9)-(11).

$$P_{\uparrow\downarrow} = \left(\hbar \frac{1}{4\pi\varepsilon r^2} \frac{\sigma\upsilon}{|e|\omega\lambda}\left(\frac{u_\tau}{u}\right)\right)^2 \left[\frac{\sigma_0}{\frac{\nu}{\lambda}\sqrt{\frac{\rho}{\tau}}}\right] \tag{12}$$

The quantity called spin diffusion distance, as previously stated, is the constraint in terms of distance for the diffusion of a particle spin. According to (Doornenbal, 2018), λ can be assumed as the quotient between the velocity and local vorticity of the fluid, as stated by Equation (13).

$$\lambda = \frac{u}{\Omega} \tag{13}$$

Furthermore, by using salt water as the working fluid, the vorticity is considered as equal to the linear velocity, given that the viscosity of salt water has is lower than that of liquid Gallium.

However, due to the degree of purity of salt water, in comparison to Gallium 99.9%, it can be considered that the spin diffusion length $\lambda_{\text{Salt water}}$ is smaller, since the path to be traveled by the spin-particle between impacts is smaller in an environment whose electron density is smaller while the number of impurities is higher. Hence, despite not being smoothed out through viscosity, the electrical and spin conductivity can decrease gradually with the exposure of the fluid to impurities, given that salt water is not a highly viscous fluid.

3. Numerical Simulation of Spin Hydrodynamics

By considering the mathematical model for the SHD energy harvesting, as stated by Equation (7), it is necessary to compute and thoroughly analyze the assumptions that are to be made in terms of microscopic quantities. Moreover, certain variables cannot be measured directly. As a result, certain approaches to assume reasonable values for them are deemed crucial.

For instance, the local vorticity is an immeasurable quantity; hence, according to (Doornenbal, 2018), the estimation of Ω can be made based on the quotient between the maximum linear velocity u and the spin diffusion distance λ, which is a reasonable assumption.

Existence of vortices is essential as spin polarizers within a certain distance until these vortices get smoothed out by the viscosity action. Hence, based on the previous conditions, **Table 1** exhibits the values assumed in the estimation of both $E_{\uparrow\downarrow}$ and $V_{\uparrow\downarrow}$.

The simulations performed for the combined model on Magneto-hydrodynamics and Spin Hydrodynamics have shown results wherein the induced electric field through both MHD and SHD can be found as a superposition across the channel section.

In the case of MHD, the magnetic field profile has been modeled as a hyperbolic cosine function in terms of magnetic flux density. Given that the developed experimental channel has rare earth permanent magnets on both sides, *i.e.* in the horizontal axis, the distribution of magnetic flux density becomes more intense due to the proximity to the magnetic poles. This enables the action of the Lorentz force over the charged particles on both sides of the channel. In addition, the higher the permanent magnets' grade, the more intense its magnetic remanence becomes. It turns out that, for strong magnetic fields, the effects of MHD

Table 1. Considered parameters.

Parameter	Unit	Magnitude
Channel Length (Y)	m	0.154
Electrical Conductivity (σ_{Ga})	S/m	3.861×10^{6}
Electrical Conductivity ($\sigma_{\text{Salt water}}$)	S/m	27.954
Dynamic Viscosity (μ_{H_2O})	Pa.s	9.6×10^{-4}
Dynamic Viscosity (μ_{Ga})	Pa.s	1.879×10^{-3}
Spin Diffusion Length (λ_{Ga})	m	1×10^{-8} [1]
Spin Diffusion Length ($\lambda_{\text{Salt water}}$)	m	1×10^{-9}
Distance between electrodes (r)	m	0.04
Planck's Constant (h)	J.s	6.62×10^{-34}
Electrical Permittivity (ε)	F/m	8.85×10^{-12}
Local Vorticity (Ω_{Ga})	1/s	2.154×10^{4}
Local Vorticity ($\Omega_{\text{Salt water}}$)	1/s	0.7158
Maximum Linear Velocity (u)	m/s	1.7382
Elementary Charge (e)	C	1.6×10^{-19}
Maximum Electric Field (NaCl)—SHD	N/C	0.08
Maximum Electric Field (Ga)—SHD	N/C	0.2
Maximum Voltage (NaCl)—SHD	V	0.004825
Maximum Voltage (Ga)—SHD	V	0.008

over the flowing charged particles become more noticeable.

However, in the absence of magnetic field, the effects of SHD may have a rise due to a non-biased occurrence of the Inverse Spin Hall Effect. The term "non-biased" has been used since whenever the spin degree of freedom of charged particles is an allowed quantity in the analysis, these flowing particles may experience the Stern-Gerlach Force [9]. This is a magnetic force just like the Lorentz force, yet it only represents the interaction of the particles' spin and the external magnetic field, and not the influence of an electric charge in motion across magnetic flux lines.

The simulation results under conditions of absence, low, and relatively high magnetic field applied through the ionized fluid flow are illustrated in **Figure 6(a)-(left)**, **Figure 6(a)-(middle)** and **Figure 6(a)-(right)** when liquid Gallium is utilized, while **Figure 6(b)-(left)**, **Figure 6(b)-(middle)** and **Figure 6(b)-(right)** show patterns of electric field for salt water as the working fluid.

4. Experimental Results on SHD Energy Harvesting

It is necessary to build an experimental set up to provide a way of measuring and proving the quantities predicted according to the developed model. Consistency

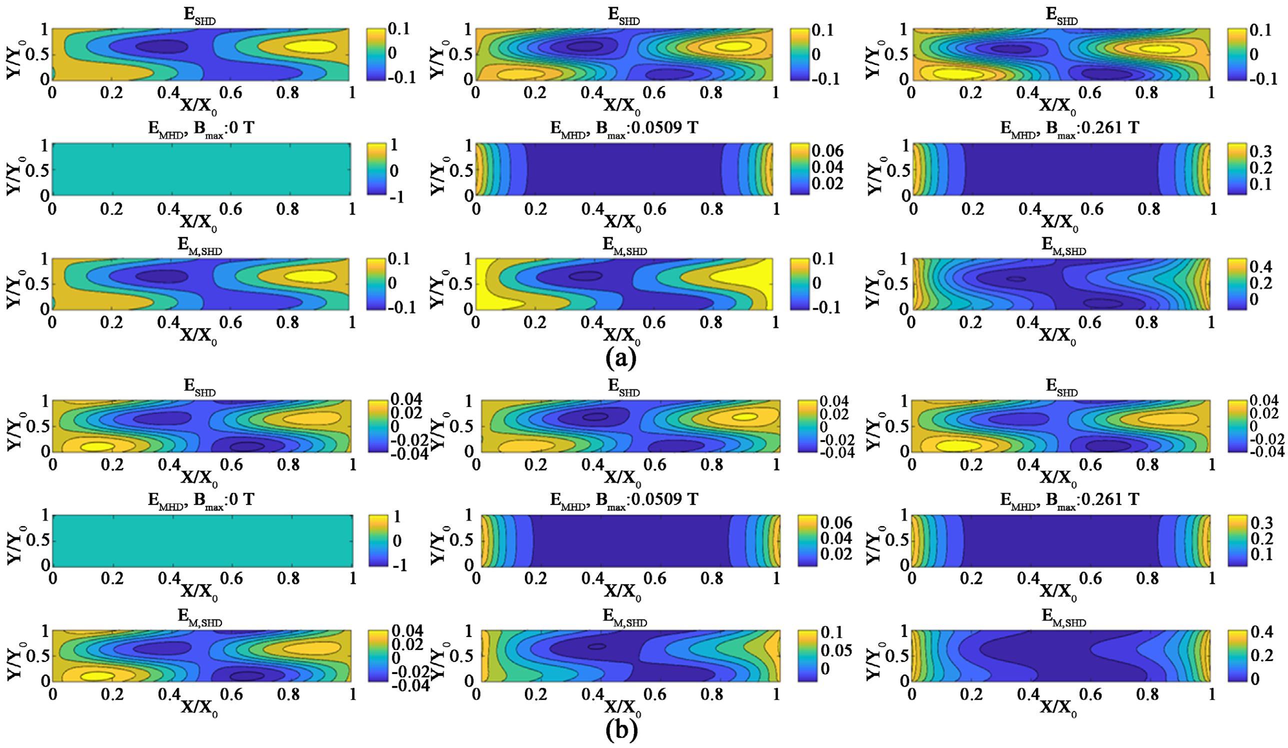

Figure 6. (a) (left) Electric field induced in liquid Gallium when $B = 0$ T, (middle) $B = 0.05090$ T and (right) $B = 0.261$ T; (b) (left) Electric field induced in salt water when $B = 0$ T, (middle) $B = 0.05090$ T and (right) $B = 0.261$ T

in this regard plays a fundamental role, given that Spin Hydrodynamics is a field that yet to be figured out and had its first experimental results reported by *Takahashi et al.* in 2016.

Our analysis reveals a clear difference between the reported results by (Baerends, 2018) and (Takahashi, 2016), some of which differ with more than three orders of magnitude. Furthermore, the experimental results obtained by our research group will be described in detail, comprising the observations and eventual effects that may interfere in the acquisition of those patterns ascribed as the signature of SHD effects through a fluid flow.

Measurements have been made by using the FLUKE 116 True Rms, Oscilloscope Infiniium DSO9404A—Agilent Technologies with High resolution, tuned for a 10mV scale, timescale from −10.0 to +10.0 seconds and a sampling frequency of 5 kHz for all tests.

4.1. Configuration with a Single Resistive Load

For this procedure, a single resistor of 178.4 Ω has been placed in one of the sides of the rectangular channel. In addition, the volume of fluid has been fixed to 1000 mL with a saline concentration of 200 g/L of Sodium Chloride.

Notably, the same experiment was performed ten times for accuracy and consistency checks. Figure 3 illustrates the sketch of the system connections and graphically depicts the fluid velocity profile and development of boundary layer thickness [15]. The fluid flow in close vicinity of the channel walls are more susceptible to the shear stress induced by the fluid-structure interaction.

This arrangement creates a region in which the likelihood of triggering vortices is larger than any other region across the channel section. As described in [1], angular velocity and vortices exert a direct influence over spin particles, thereby inducing spin polarization through the Inverse Spin Hall Effect.

As an example, **Figure 7** exhibits how the development of a boundary layer increases the likelihood of vortices' triggering and, consequently, to the voltage induction across the electrodes connected to an external load.

According to the predictions, whenever the saline fluid starts flowing throughout the channel, there is a bump in voltage measured over the resistive load, whose maximum amplitude is approximately 5.7 mV. Its waveform witnesses some smoothing process whenever the fluid is poured in the pipe. It might also occur due to the turbulence in the beginning of the flow period.

In addition, as part of the exclusion tests, both probes have been inverted in order to prove the data truly represent SHD effects and to determine whether the voltage over the resistive load would invert as well. It has been noticed that the voltage has its magnitude inverted, as expected. Due to the conditions imposed on the fluid flow, the voltage is induced across the sidewalls of the channel from a spin accumulation in close vicinity to them due to the shear stress and posterior vorticity induction in the fluid.

Figure 8 shows the obtained results for both direct and inverse connections of

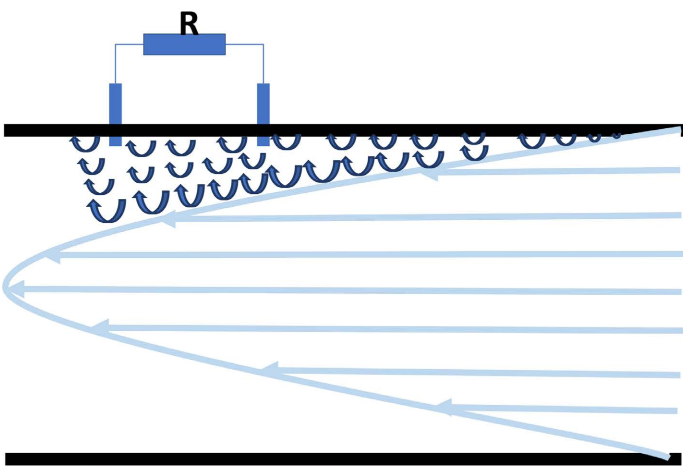

Figure 7. Single-loaded SHD energy harvesting prototype.

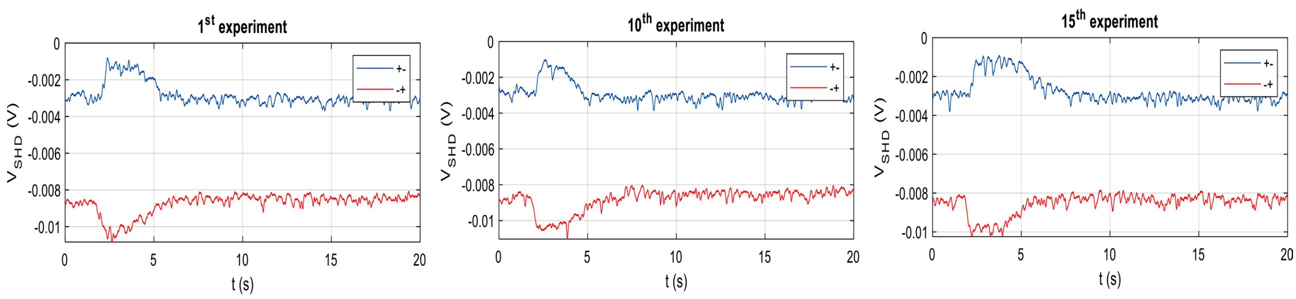

Figure 8. (left) 1st, (middle) 10th and (right) 15th experiments' results @ $R = 178.4\ \Omega$.

the oscilloscope probes in order to verify whether there was inversion in the polarity of the voltage induced.

In comparison with the previously performed procedures, the results look consistent in regards to the waveform upon the insertion of fluid into the channel (voltage spike in the very beginning of the fluid flow until the volume/second of H_2O + NaCl decays to zero). Moreover, the amplitudes achieved through the experiments are between 4 and 6.2 mV, which demonstrates how the velocity of the flow does exert influence (the same NaCl concentration has been kept throughout the all procedures).

For the sake of consistency, 40 tests were performed: 25 with the oscilloscope probes placed in the order positive-negative, which implies that + has been connected in the upper electrode and, the negative, to the lower electrode. Notably, both electrodes have been connected to resistive load whose value was mentioned above.

In addition, 15 experiments were performed with the inverted orientation of the electrodes. This has been done to show the waveform pattern remained the same.

According to the Inverse Spin Hall Effect, as the fluid flows (as well as the electrically charged particles), spin "up" and "down" particles are dragged to the vicinities of the walls, thus characterizing a transversal effect to the linear velocity direction. Hence, as spin "up" and "down" particles are located in close vicinity to the walls and copper electrodes connected to the resistive load spin difference induce a local potential difference. This, in turn, causes induction of a spin current density in that region, which typically works similar to a DC power source.

It is noteworthy that the voltage signal acquired experimentally is not continuous due to the factors mentioned as follows: 1) limited volume of fluid inserted throughout the channel, 2) as the flow ceases to exist, it no longer maintains linear velocity, angular velocity, or vorticity, and 3) velocity fluctuations make the signal noisy, since the vorticity depends on the linear velocity and its time variation.

The voltage pattern remains the same for all of the experiments. Nonetheless, the voltage bump changes in accordance with the transient of fluid insertion in the pipe. It has been noticed that voltage decay time varies between 1.8 to 4 seconds. This time variation occurs due to the local vorticity which changes over time. However, this parameter requires statistical analysis for an approximate value. Lastly, the positioning of electrodes throughout the channel walls impacts the vorticity distribution as well since these components have a saliency towards the center of the channel.

4.2. Parallel Configuration of Two Resistive Loads

Next, the experimental setup has been adjusted for a 2-resistive load configuration, whose resistors were connected in opposite sides of the pipe in parallel.

Those values are178.5 Ω and 177.5 Ω, respectively, also comprising of resistor and wire connections to the measurement probes.

The distance between the electrodes connected to each of these resistors is equal to 40 mm and, for this procedure; the chosen sampling frequency was 2.5 kHz. In addition, the fluid fixed volume is equal to 1000 mL, whose saline concentration reaches 200 g of Sodium Chloride per liter of water.

This procedure was repeated ten times for the sake of consistency and accuracy validation. The experimental setup sketch is shown in **Figure 9** in order to clarify the configuration of the resistive loads and development of a boundary layer thickness due to the shear stress between fluid and channel structure, which ends up inducing vorticity and, in effect, creating the possibility of orienting spin particles through the spin-orbit coupling [20].

Two resistors have been placed in opposite sides of the pipe to determine the effects of a SHD system subject to approximately two equal external loads. In addition, the oscilloscope probes have been positioned as a mirror setup, just by repeating the same polarity of the probes placed on the opposite wall.

Moroever, both resistors have the same voltage signal, as their configurations regarding connections with the oscilloscope probes are the same. The experimental results exhibited what had been expected using the theoretical model. The voltage patterns for the parallel configuration can be illustrated in **Figure 10**.

Positive voltage spikes over both loads upon fluid injection throughout the channel. Afterwards, the voltage signal is shown to build up more softly over R2, while the same phenomena occur for R1. Despite apparent irregularities and chaotic behavior in the fluid flow, the symmetry condition assumed in the mathematical model is observed through the experimental procedure.

Besides, it is important to highlight the voltage builds up more rapidly than it decays. This can be attributed to the time constant of the fluid associated with its resistance and capacitance, as well as the reduction of the volume per second of fluid.

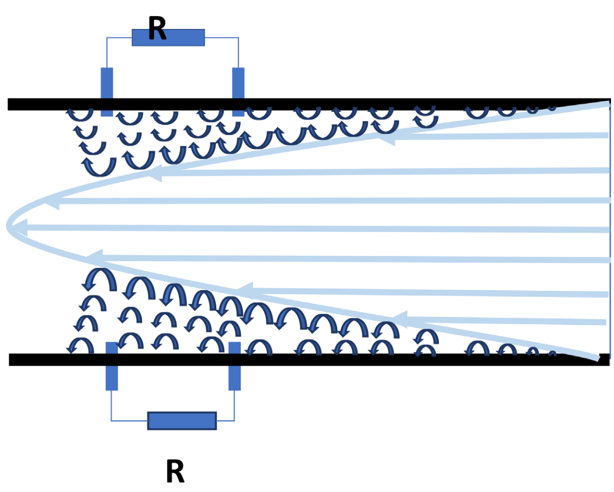

Figure 9. Parallel loaded SHD energy harvesting prototype.

4.3. Series Configuration of Resistive Loads

In the third procedure, two resistive loads have been placed on the same side of the channel. Their values, comprising of the resistance itself and wires used for connections are, 178.5 Ω and 177.5 Ω, respectively. The distance between the electrodes is equal to 40 mm.

Furthermore, the utilized volume of fluid equals 1000 mL with a saline concentration equivalent to 200 grams of Sodium Chloride per liter of water. This experiment was repeated ten times to ensure accuracy and consistency. Figure 11) illustrates the sketch of the experimental setup that was used to verify forecasted phenomena regarding the electric current density induction through spin-orbit coupling of the flowing particles.

For this test, R1 and R2, CH1, and CH2 have been connected on the same side of channel. The voltage over R1 is a positive pulse which lasts about 15 seconds, according to the second test. R2's voltage pulse has, in principle, the same duration, but it can be observed that the polarity of the signal is negative, opposing the R1's voltage pulse.

In addition, V2 has a smoother decay as compared to the rise of V1, which experiences a radical increase upon the commencement of the fluid flow. At the end of the pulses, the first situation switches sides: V2 has a sharp increase towards the offset value. Meanwhile, V1 has a smoother decay back to its offset. In some cases, V2 has either rises softly or decays, depending on how the fluid flow

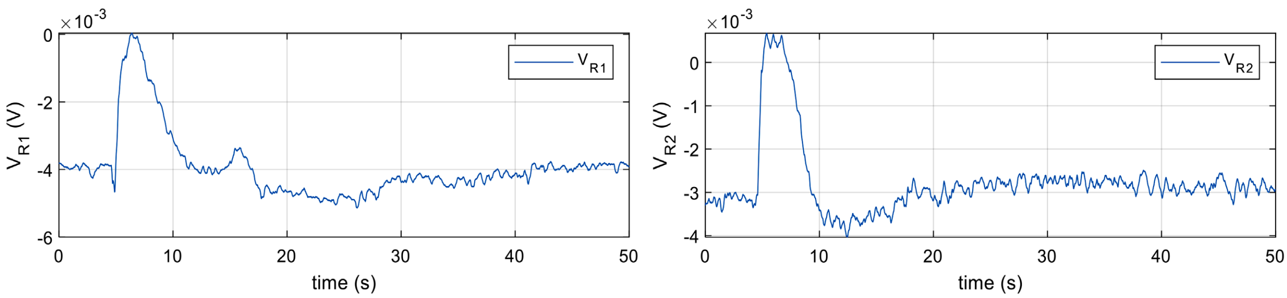

Figure 10. Parallel loaded SHD energy harvesting prototype.

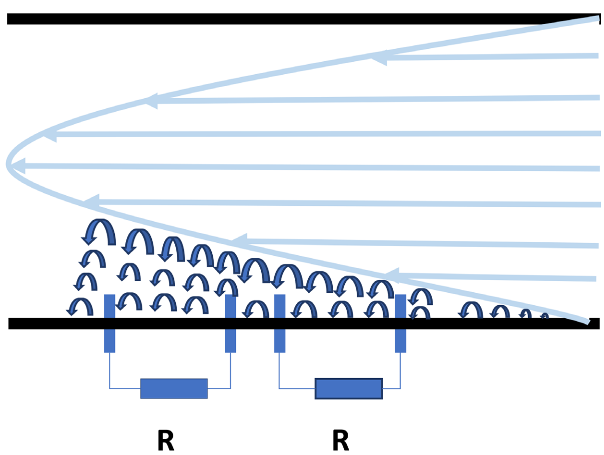

Figure 11. Loads on the same side of the SHD energy harvesting prototype.

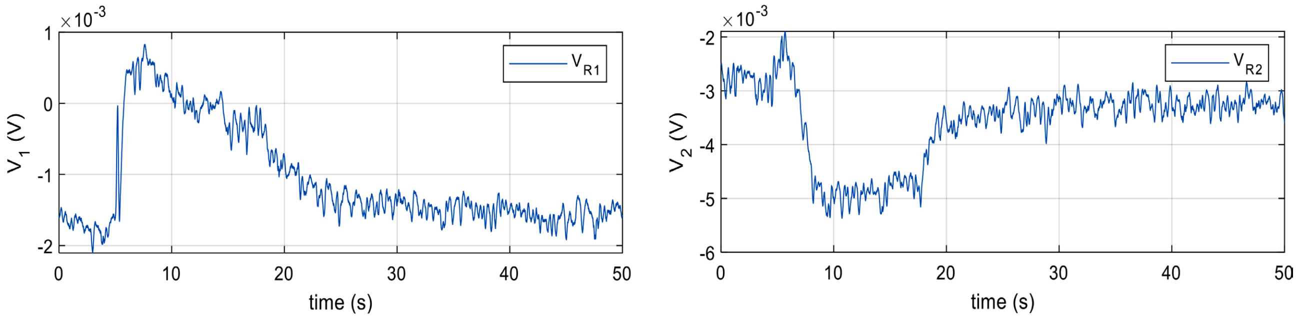

Figure 12. Potential difference over (left) R1 and (right).

starts and gets extinguished. **Figure 12** shows how the voltage variation across the terminals of each resistive load develops upon the insertion of a conductive fluid.

Upon fluid injection through the channel, spikes are observed in either R1 or R2 voltages. Both reveal a positive voltage spike in the very beginning of the fluid flow, but the V1 keeps at the peak value and starts decaying after that transient. V2 exhibits the same pattern, albeit with the opposite polarity.

5. Conclusion

Throughout the phases of this investigation, the prototype has been setup, calculations regarding basic conditions of operation for energy conversion purposes have been performed to verify whether the phenomena regarding Spin Hydrodynamics could be observed at room temperature. These validation tests encompassed vital information for the progress of the first level in this research project. Different resistive loads and configurations were tested along with mathematical models in order to accurately describe Spin Hydrodynamics and to provide a reasonable forecast of results obtained. In addition to the validation tests and phenomenological analysis, the so-called exclusion tests were also performed continuously with a view to certify the fact that there was no data contamination. Firstly, procedures were performed to verify the accuracy and reliability of data and to test the effects of Spin Hydrodynamic generation. Furthermore, thermal effects are found to be negligible since all procedures have been performed at room temperature, given that no cooling or heating device has been used, thus excluding the possibility of observation of the Seebeck Effect. Moreover, there is no risk of exposing the prototype to the external electric field, since the channel is made of plastic material. Lastly, unlike MHD Generators, the measured voltage is contingent on the length of the channel, thereby endorsing the action of Spin polarization due to Spin-Orbit Coupling, as a consequence of the Inverse Spin Hall Effect (ISHE).

Conflicts of Interest

The authors declare no conflicts of interest regarding the publication of this paper.

References

[1] Takahashi, R., Matsuo, M., Ono, M., Harii, K., Chudo, H., Okayasu, S., Ieda, J., Takahashi, S., Maekawa, S. and Saitoh, E. (2015) Spin Hydrodynamic Generation. *Nature Physics*, **12**, 52-56. https://doi.org/10.1038/nphys3526

[2] Žutić, I., Fabian, J. and Das Sarma, S. (2004) Spintronics: Fundamentals and Applications. *Reviews of Modern Physics*, **76**, 323-410. https://doi.org/10.1103/RevModPhys.76.323

[3] Meyer, S., *et al.* (2017) Observation of the Spin Nernst Effect. *Nature Materials*, **16**, 977-981. https://doi.org/10.1038/nmat4964

[4] Sato, K. and Saitoh, E. (2015) Spintronics for Next Generation Innovative Devices. John Wiley & Sons, Ltd., Hoboken. https://doi.org/10.1002/9781118751886

[5] Mitofsky, A.M. (2018) Direct Energy Conversion.

[6] Davidson, P.A. (2001) An Introduction to Magnetohydrodynamics. Cambridge University Press, Cambridge. https://doi.org/10.1017/CBO9780511626333

[7] Lipscombe, G., Penney, J., Leyser, R. and Allison, H.J. (2014) Water under the Bridge. Department of Physics and Astronomy, University of Leicester, Leicester, LE17RH.

[8] Status and Perspectives of MHD Generators (1983) L. H. Th Rietjens. (Phys. Bl. 39, Nr. 7) Eindhoven.

[9] Wennerström, H. and Westlund, P. (2017) A Quantum Description of the Stern-Gerlach Experiment. *Entropy*, **19**, 186. https://doi.org/10.3390/e19050186

[10] Wen, M., Bauke, H. and Keitel, C. (2016) Identifying the Stern-Gerlach Force of Classical Electron Dynamics. *Nature Scientific Reports*, **6**, Article No. 31624. https://doi.org/10.1038/srep31624

[11] D'yakonov, M. and Perel', V. (1971) Possibility of Orienting Electron Spins with Current. *Soviet Journal of Experimental and Theoretical Physics Letters*, **13**, 657-660.

[12] Ciudad, D. (2015) Turbulent Power. *Nature Materials*, **14**, 1188. https://doi.org/10.1038/nmat4499

[13] An Internet Book on Fluid Dynamics: Poiseuille Flow. Brennen.caltech.edu. http://brennen.caltech.edu/fluidbook/basicfluiddynamics/Navierstokesexactsolutions/poiseuilleflow.pdf

[14] Zou, H., *et al.* (2019) Quantifying the Triboelectric Series. *Nature Communications*, **10**, Article No. 1427. https://doi.org/10.1038/s41467-019-09461-x

[15] Pope, V. (2000) Turbulent Flows. Cambridge University Press, Cambridge. https://doi.org/10.1017/CBO9780511840531

[16] Wu, J., Ma, H. and Zhou, M. (2006) Vorticity and Vortex Dynamics. Springer, Berlin, 255-321. https://doi.org/10.1007/978-3-540-29028-5_6

[17] Matsuo, M., Ieda, J., Saitoh, E. and Maekawa, S. (2011) Effects of Mechanical Rotation on Spin Currents. *Physical Review Letters*, **106**, Article ID: 076601. https://doi.org/10.1103/PhysRevLett.106.076601

[18] Žutić, I. and Matos-Abiague, A. (2015) Cause a Stir. *Nature Physics*, **12**, 24-25. https://doi.org/10.1038/nphys3572

[19] Matsuo, M., Ohnuma, Y. and Maekawa, S. (2017) Theory of Spin Hydrodynamic Generation. *Physical Review B*, **96**, 020401(R). https://doi.org/10.1103/PhysRevB.96.020401

[20] Saitoh, E., Ueda, M., Miyajima, H. and Tatara, G. (2006) Conversion of Spin Cur-

rent into Charge Current at Room Temperature: Inverse Spin-Hall Effect. *Applied Physics Letters*, **88**, Article ID: 182509. https://doi.org/10.1063/1.2199473

[21] Doornenbal, R., Polini, M. and Duine, R. (2019) Spin-Vorticity Coupling in Viscous Electron Fluids. *Journal of Physics*: *Materials*, **2**, Article ID: 015006. https://doi.org/10.1088/2515-7639/aaf8fb

[22] Baerends, A. (2018) Phenomenological Theory of Spin Hydrodynamic Generation. BSc, Utrecht University, Utrecht.